# Effect of instantaneous frequency glides on interaural time difference processing by auditory coincidence detectors

Brian J. Fischer[a,b,1], Louisa J. Steinberg[c], Bertrand Fontaine[d,e], Romain Brette[d,e], and Jose L. Peña[c,2]

[a]Group for Neural Theory, Département d'Etudes Cognitives, Ecole Normale Supérieure, 75005 Paris, France; [b]Laboratoire de Neurosciences Cognitives, Institut National de la Santé et de la Recherche Médicale U960, 75005 Paris, France; [c]Dominick P. Purpura Department of Neuroscience, Albert Einstein College of Medicine, Bronx, NY 10461; [d]Laboratoire Psychologie de la Perception, Centre National de la Recherche Scientifique, Université Paris Descartes, 75005 Paris, France; and [e]Equipe Audition, Département d'Etudes Cognitives, Ecole Normale Supérieure, 75005 Paris, France

Edited by Terrence J. Sejnowski, The Salk Institute for Biological Studies, La Jolla, CA, and approved September 27, 2011 (received for review June 2, 2011)

**Detecting interaural time difference (ITD) is crucial for sound localization. The temporal accuracy required to detect ITD, and how ITD is initially encoded, continue to puzzle scientists. A fundamental question is whether the monaural inputs to the binaural ITD detectors differ only in their timing, when temporal and spectral tunings are largely inseparable in the auditory pathway. Here, we investigate the spectrotemporal selectivity of the monaural inputs to ITD detector neurons of the owl. We found that these inputs are selective for instantaneous frequency glides. Modeling shows that ITD tuning depends strongly on whether the monaural inputs are spectrotemporally matched, an effect that may generalize to mammals. We compare the spectrotemporal selectivity of monaural inputs of ITD detector neurons in vivo, demonstrating that their selectivity matches. Finally, we show that this refinement can develop through spike timing-dependent plasticity. Our findings raise the unexplored issue of time-dependent frequency tuning in auditory coincidence detectors and offer a unifying perspective.**

barn owl | nucleus laminaris

Interaural time difference (ITD) is a primary cue for detecting the horizontal position of a sound source (1, 2). The most prevalent model for the mechanism underlying ITD sensitivity assumes that it is created by a circuit of neural delay lines and coincidence detector neurons (3–6). In this model, coincidence detector neurons respond when the left and right ear inputs arrive nearly simultaneously. The temporal delays of the left and right ear inputs created by axonal delay lines determine the neuron's best ITD. An alternative theory retains the coincidence detectors responding to delayed binaural inputs, but postulates cochlear delays instead (7). Experimental evidence in birds does not support this alternative theory (8–10), although some studies in mammals are consistent with it (11). In mammals, ITD sensitivity is thought to be established by the timing of both excitatory and inhibitory inputs (12).

A fundamental question these models raise is whether the monaural inputs to the binaural coincidence detector neurons differ only in their timing. Though current evidence is consistent with identical bilateral input shifted in time (5, 8–10, 13), analyses have not taken into account the selectivity of early auditory neurons for the time-dependent spectral structure of sound, which can arise in the auditory nerve.

In the mammalian auditory nerve, neurons display a change of preferred instantaneous frequency with time (14–17). This response property is characterized by an instantaneous frequency (IF) glide in the neuron's impulse response. IF glides are also seen in the local field potentials in the owl's nucleus laminaris (NL) (18). It is unknown whether neurons in NL or medial superior olive (MSO), the first binaural nuclei in the avian and mammalian ITD processing pathways, respectively, are selective for these spectrotemporal features and how such selectivity may affect the processing of ITD (4–6). Here, we show selectivity for IF glides of neurons in the owl's NL and their input from the cochlear nucleus magnocellularis (NM). We show that mismatching the left and right inputs can dramatically affect ITD processing. Finally, we examine the spectrotemporal selectivity of the left and right inputs of individual NL neurons recorded in vivo. We demonstrate that selectivity to IF glides matches bilaterally, and that this refinement can develop through spike timing-dependent plasticity (STDP).

## Results

**Frequency Glides in Impulse Responses of NL Neurons and Their Input.** Impulse responses of single neurons were estimated from responses to broadband noise bursts using the spike-triggered average (STA) (19, 20). Impulse responses of single units in the input to NL, axons of nucleus magnocellularis (NM) neurons, and NL neurons show an IF glide. We fit the STAs with chirping and nonchirping filters, where the chirping filters had a linear IF glide (Eqs. **1–4**). STAs were better fit by the chirping filters than by the nonchirping filters (Fig. 1; in NM and NL, Mann–Whitney $U$ test, $P < 0.02$ in both cases). This finding is consistent with a previous analysis of the neurophonic in NL (18). In contrast to this study, we found no significant difference between the fits provided by the gammachirp and gaborchirp filters (Fig. 1 $E$ and $F$; NM, $n = 57$, median gammachirp $\chi^2 = 1.71$, median gaborchirp $\chi^2 = 1.60$, $P = 0.24$; NL, $n = 27$, median gammachirp $\chi^2 = 2.11$, median gaborchirp $\chi^2 = 1.99$, $P = 0.92$; Mann–Whitney $U$ test). Below, we describe the fits obtained with the gammachirp filter.

A range of gammachirp filter parameters was observed at each best frequency (BF; Fig. 2). Our estimate of the neuron's BF was the frequency with largest power in the Fourier transform of the gammachirp fit, which is equivalent to the tone producing the largest response for a cross-correlator neuron. The instantaneous frequency at the initial time $f_0$ was highly correlated with BF in both NM and NL (Fig. 2 $A$ and $B$; $r^2 = 0.99$, $P < 10^{-3}$ in NM and $r^2 = 0.98$, $P < 10^{-3}$ in NL). The IF glide slope was positively correlated with the BF of the neuron in both NM and NL (Fig. 2 $C$ and $D$; $r^2 = 0.43$, $P < 10^{-3}$ in NM and $r^2 = 0.45$, $P < 10^{-3}$ in NL). Fig. 2 illustrates that, although correlated, the IF glide slope varied across neurons with similar BF. The time constant

Author contributions: B.J.F. and J.L.P. designed research; B.J.F., L.J.S., and J.L.P. performed research; B.J.F., B.F., R.B., and J.L.P. analyzed data; and B.J.F., L.J.S., B.F., R.B., and J.L.P. wrote the paper.

The authors declare no conflict of interest.

This article is a PNAS Direct Submission.

[1]Present address: Department of Mathematics, Seattle University, Seattle, WA, 98122.

[2]To whom correspondence should be addressed. E-mail: jose.pena@einstein.yu.edu.

This article contains supporting information online at www.pnas.org/lookup/suppl/doi:10.1073/pnas.1108921108/-/DCSupplemental.

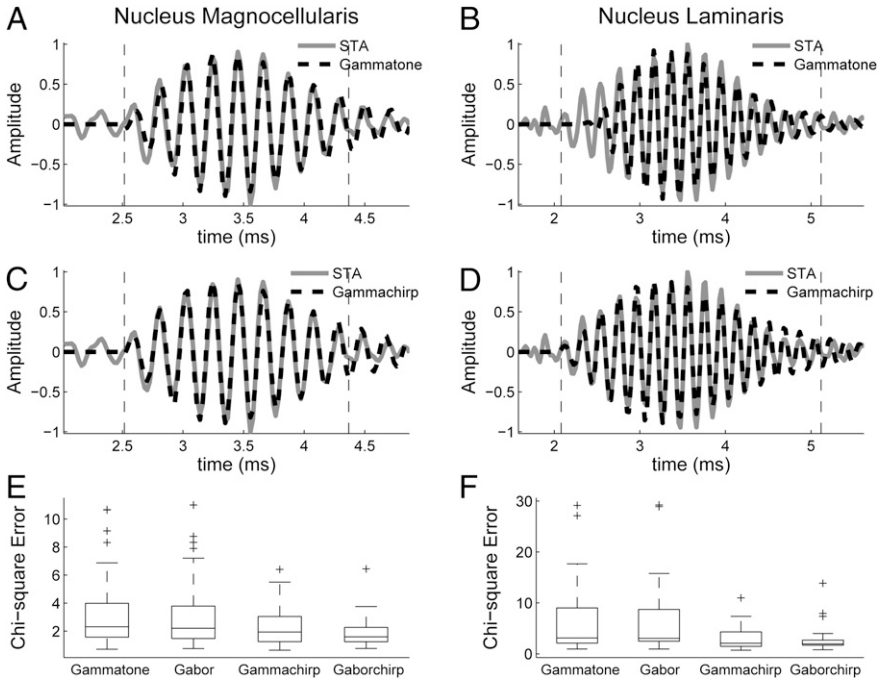


**Fig. 1.** (*A–D*) Example fits of the spike-triggered average (STA) in nucleus magnocellularis (NM) and nucleus laminaris (NL) with gammatone (*A* and *B*) and gammachirp (*C* and *D*) filters. The dotted lines mark the interval where the envelope of the STA exceeded 10% of the maximum value. (*E* and *F*) Summary $\chi^2$ errors for fits of NM (*E*) and NL (*F*) STAs with gammatone, gabor, gammachirp, and gaborchirp filters.

of the gammachirp filter was not correlated with BF in NM and was weakly negatively correlated with BF in NL ($r^2 = 0.04$, $P = 0.16$ in NM and $r^2 = 0.22$, $P = 0.014$ in NL). Thus, the inputs to ITD-sensitive neurons in NL have IF glides whose parameters vary over a broad range. The question thus arises of how these additional dimensions of response selectivity affect ITD processing.

**ITD Shifts Caused by Mismatched Spectrotemporal Inputs to NL.** We considered the effect of the IF glide on the encoding of ITD using a cross-correlation model of ITD-sensitive neurons (13, 21, 22). We examined the effect of interaural mismatches in the time constant $\tau$ and the IF glide slope $c$ of the monaural input filters on the best ITD of neuron. For a given BF, we modeled neurons with input filters having combinations of $\tau$ and $c$ that cover the observed range in NM, but with identical temporal and phase delays. We found that small mismatches in $\tau$ and $c$ can cause the neuron's best ITD to vary between approximately −1,000 μs and 1,000 μs (Fig. 3). This range is far larger than the owl's physiological ITD range (2, 23). The best ITD is more highly correlated with $\Delta\tau$, than with $\Delta c$. However, changes in either $\Delta c$ or $\Delta\tau$ can produce changes in best ITD that are significant for the owl's physiological range. Matching of monaural spectrotemporal filters can thus be a dramatic determinant of ITD tuning.

**Spectrotemporal Matching of Inputs to NL Neurons.** To test whether spectrotemporal properties of monaural inputs influence ITD tuning in NL neurons, we measured these parameters in NL neurons ($n = 20$) recorded in vivo. We computed the effective monaural inputs to NL neurons as the left- and right-side STAs using responses to binaurally uncorrelated noise (13). We then fit the monaural STAs with gammachirp filters to characterize their spectrotemporal properties. The parameters of the left and right gammachirp filters were highly correlated (Fig. 4). The left and right $f_0$ values were highly correlated (Fig. 4*B*; $n = 20$; $r^2 = 0.98$, $P < 10^{-3}$), as were the left and right IF glide slopes (Fig. 4*D*; $n = 20$; $r^2 = 0.51$, $P < 10^{-3}$). For the entire population, the left and right time constants showed weak, although significant, correlation (Fig. 4*F*; $n = 20$; $r^2 = 0.20$, $P = 0.05$). After removing the two outliers, the left and right time constants were highly correlated ($n = 18$; $r^2 = 0.57$, $P < 10^{-3}$). Thus, the monaural inputs to NL neurons are matched for spectrotemporal properties.

Differences in timing and phase between the two monaural inputs largely determined the observed best ITD (Fig. 4*G*). We ran the model with experimentally determined gammachirp filters to test whether mismatches influence the ITD tuning. The best ITD of neurons computed using the measured parameters was highly correlated with the best ITD computed when the time

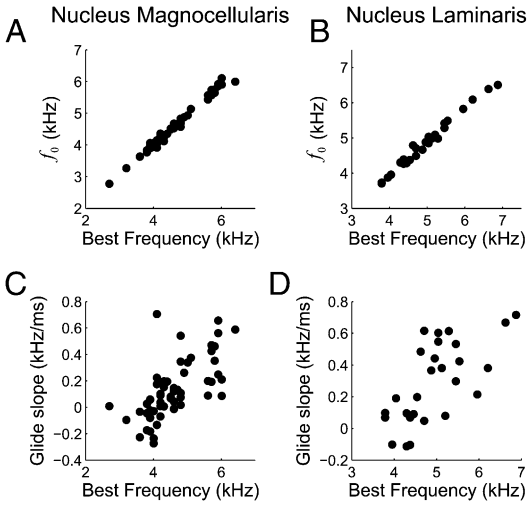


**Fig. 2.** Initial instantaneous frequency (*A* and *B*) and instantaneous frequency glide slope (*C* and *D*) parameters of the gammachirp filter fit to STAs as a function of best frequency in NM (*A* and *C*) and NL (*B* and *D*). Note the different ranges used for axes in the NM and NL plots.

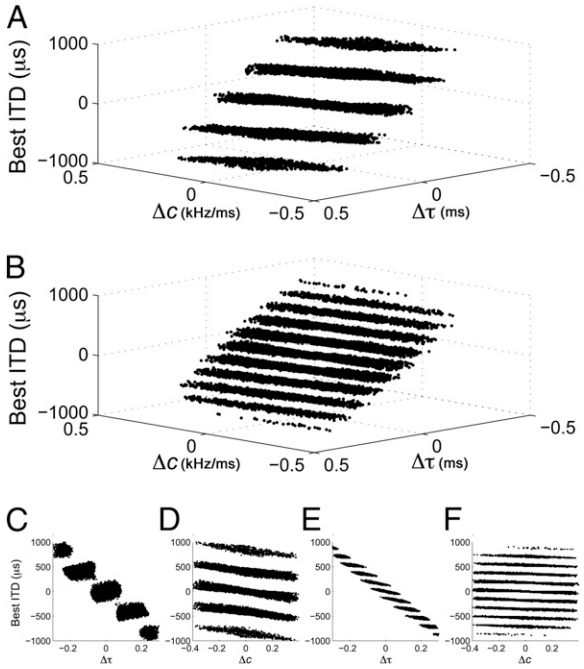


**Fig. 3.** ITD shifts produced by mismatching the spectrotemporal tuning of monaural inputs to simulated cross-correlator neurons. (*A* and *B*) ITD shifts in cross-correlator neurons with best frequency 2 kHz (*A*) and 6 kHz (*B*) when the monaural IF glide slope $c$ and time constant $\tau$ are mismatched. The distribution of datapoints in parallel layers is because of the periodic response to ITD. (*C*–*F*) Corresponding plots for $c$ and $\tau$ at 2 kHz (*C* and *D*) and 6 kHz (*E* and *F*).

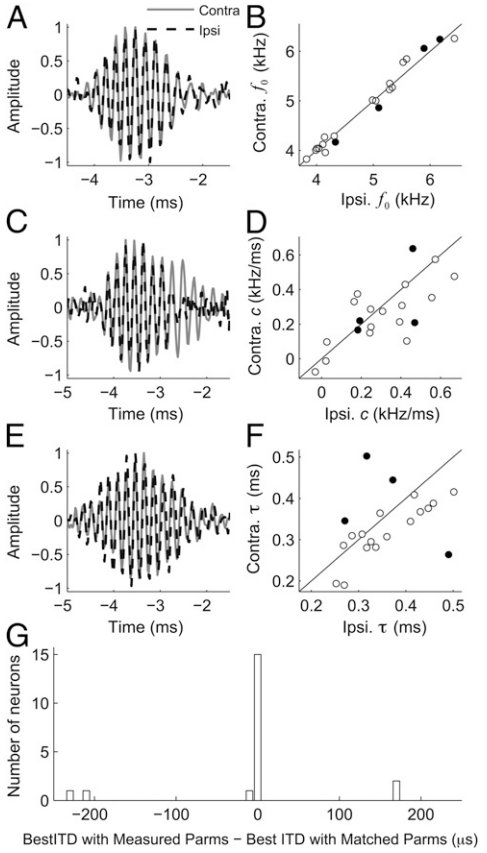


**Fig. 4.** Spectrotemporal matching of monaural inputs to NL neurons. (*A*, *C*, and *E*) Example left and right STAs for three NL neurons. (*B*, *D*, and *F*) Parameters of gammachirp fits ($f_0$, $c$, $\tau$) to left and right STAs of NL neurons. (*G*) Comparison of best ITD of NL neurons computed by a cross-correlation model when left and right IF glides are as measured or made to match. The difference indicates the amount of the best ITD that is because of differences in the IF glide. In four neurons, removing the mismatch resulted in a large difference between measured and predicted ITD. The parameters of the gammachirp fits of these four neurons are indicated by black circles in *B*, *D*, and *F*.

constant, IF glide slope, and $f_0$ were made equal ($r = 0.99$, $P < 10^{-3}$). Thus, for most neurons, interaural differences in delay and phase are sufficient to determine the best ITD. However, four neurons had large interaural mismatches in the time constant, or the IF glide slope (black circles; Fig. 4 *B*, *D*, and *F*). For these neurons, removing the mismatches in IF glides created a shift in best ITD of ~200 μs (Fig. 4*G*).

Remarkably, cross-correlation of the left and right STAs predicted ITD tuning in all NL neurons, including neurons with unmatched monaural STAs. We assessed ITD tuning by measuring rate-ITD tuning curves using broadband noise ($n = 6$) and tuning to interaural phase difference (IPD) varying stimulating frequency ($n = 7$) in independent subsets of neurons. IPD was computed by converting time differences into phase difference for a given stimulating frequency. As shown previously, the cross-correlation model predicts accurately the rate-ITD tuning curves for noise ($r^2 = 0.85 \pm 0.05$) (13) and the IPD vs. stimulating-frequency relationships ($r^2$, median = 0.47, range 0.07–0.83; Fig. 5). All neurons had nonlinear IPD vs. stimulating-frequency relationships (24). However, the root mean square (RMS) error in the linear approximation was small for all neurons (median RMS error 0.028 cycles, range 0.018–0.044 cycles). These results demonstrate that the monaural STAs are a faithful estimate of the monaural input to NL neurons.

**Learning Bilateral Spectrotemporal Matching.** We consider a learning rule to achieve the high precision of the binaural matching, where synaptic modification is determined by the difference in timing of postsynaptic and presynaptic spikes, at each synapse. Such an STDP mechanism has been demonstrated in many preparations (25, 26), in particular in the auditory system (27). It has been shown that STDP can account for the development of ITD-sensitive neurons (28–30). However, these studies addressed only the learning of temporal delays. Here, we test whether STDP could lead to binaural matching when the input parameter space is more complex: in addition to the standard axonal delay axis, the input filters have three additional degrees of freedom: the starting frequency $f_0$, the glide slope $c$, and the time constant $\tau$. To test this hypothesis, we simulated the development of binaural neurons fed by shifted white noise signals at the ears. Initially, 150 NL neurons received synaptic inputs from 150 monaural NM neurons on both sides. Each input neuron is characterized by a triplet of gammachirp parameters ($f_0$, $c$, and $\tau$) and an axonal delay. For each input neuron, the gammachirp parameters are randomly taken from a distribution similar to the one measured in NM (Fig. 2), and the axonal delay is randomly taken between 0 and 300 μs. After the learning stabilized the firing rate and weights of the NL neurons, the STDP was switched off and the monaural STAs were computed. Twelve neurons were discarded because they yielded inputs coming only from one side or because they yielded flat STAs (*Materials and Methods*).

The resulting BFs are closely matched bilaterally (Fig. 6*A*) ($r^2 = 0.96$ compared with $r^2 = 0.96$ in the measurements; regression slopes not significantly different, $P = 0.24$, ANCOVA), a trend that was shown in previous studies (8–10). In addition, the matching of spectrotemporal parameters of the input filters show trends that are in correspondence with the measurements. The

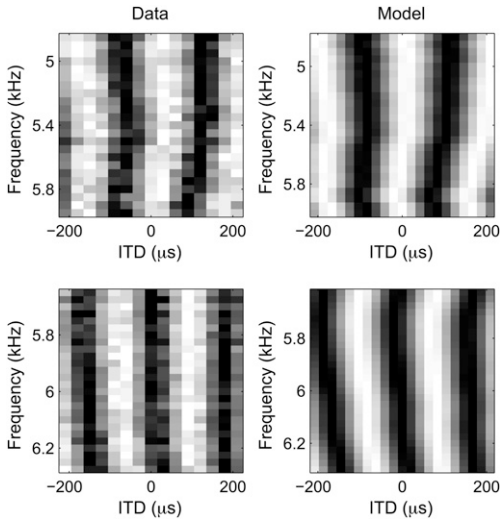


**Fig. 5.** Predicting ITD tuning. Rate ITD tuning curves for tonal stimuli measured for two NL neurons (*Left*) and predicted by the cross-correlation model (*Right*). Each tuning curve is normalized for display. White corresponds to high mean firing rate and black to low mean firing rate.

left and right $f_0$ values were highly correlated (Fig. 6*B*) ($r^2 = 0.84$ compared with $r^2 = 0.98$ in the measurements; regression slopes not significantly different, $P = 0.27$, ANCOVA). The left and right IF glide slopes were also highly correlated (Fig. 6*C*) ($r^2 = 0.49$ compared with $r^2 = 0.51$ in the measurements; regression slopes not significantly different, $P = 0.65$, ANCOVA). The left and right time constants were more weakly, although significantly, correlated (Fig. 6*D*) ($r^2 = 0.26$, compared with $r^2 = 0.20$ in the measurements; regression slopes not significantly different, $P = 0.76$, ANCOVA). There is a trend for the resulting time constants to be clustered at lower values than either the in vivo measurements or the model NM inputs. This could be due to smaller time constants inducing more temporally precise firing, a property that STDP will prefer. Also, the rising time of a filter with a smaller time constant is smaller, leading to earlier spike generation, a property that is known to be favored by STDP (31).

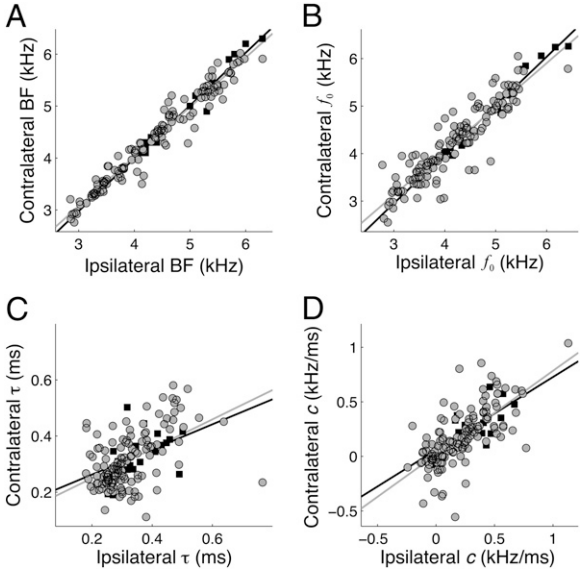


**Fig. 6.** Bilateral spectrotemporal matching produced by spike timing-dependent plasticity. (*A*) Best frequencies (BF) of the 138 left and right model NL neurons (gray circles) and 20 real NL neurons (black squares). (*B–D*) Parameters of gammachirp fits to left and right STAs of model NL neurons (gray circles) and NL neurons (black squares). Solid lines are regression lines.

## Discussion

**Frequency Glides in Early Auditory Processing.** We found that the coincidence detector neurons of the owl's NL and their input from NM tuned to IF glides. Together with other reports (14, 18), this study shows that neurons in avian and mammalian auditory systems function as similar spectrotemporal filters. The presence of IF glides in the impulse responses of peripheral auditory neurons indicates that there are parameters of response selectivity in addition to BF that must be considered in ITD detection. We show that selectivity for IF glides by binaural neurons can greatly affect ITD tuning.

**Binaural Spectrotemporal Matching and ITD Tuning.** Our analysis shows that bilateral mismatching of preferred spectrotemporal properties can significantly affect processing of ITD. Small mismatches in the IF glides of monaural inputs can account for best ITDs as large as those observed in the owl's auditory system. If mismatches in IF glides are significant determinants of ITD tuning, then neurons will show a nonlinear relationship between best IPD and stimulus frequency, and the criteria for having a characteristic delay (CD) (32, 33) would no longer apply. We found that, by virtue of matching the spectrotemporal selectivity of the left and right inputs, delay lines remain as the major factor in determining best ITD in most NL neurons. However, small mismatches found in the monaural filters of most neurons, and larger ones observed in a small minority of cells, indicate that the Jeffress model (3) does not completely describe the computation of ITD in the owl. Rather, the general principle that explains ITD tuning in all of these cells is the cross-correlation of monaural inputs (13).

Matching of monaural spectrotemporal receptive fields in binaural neurons has been shown previously (34), but neither at the site of monaural convergence nor at the time scale demonstrated here. Thus, the inputs to coincidence detector neurons are refined beyond BF, delay, and phase. The bilateral spectrotemporal matching in NL is a demanding task for input refinement, given the variability in the IF glides of NM neurons, the input to NL. We show that this level of input matching can develop according to an STDP rule. STDP has previously been shown to allow the development of ITD-sensitive neurons by selecting for particular delays and phases (28). Here we show that STDP can cause NL neurons to match the monaural input filters. The spectrotemporal matching of left and right inputs to coincidence detector neurons may represent a cost-effective mechanism. Performing coincidence detection on the output of filters based on parameters other than microsecond-accurate temporal resolution may reduce the cost of ITD detection.

**A General Mechanism for Producing Delays.** In mammals, ITD sensitivity is thought to arise from the temporal alignment of excitatory and inhibitory inputs that are precisely timed on a microsecond scale (12). The idea is that inhibitory inputs determine the neuron's best ITD by influencing the relative delays of the left and right postsynaptic potentials. The modeling work presented here allows us to suggest an alternative interpretation of these results. A systematic mismatch of monaural filter parameters could produce the dependence of best ITD on BF that is seen in the mammalian MSO (35). Impulse responses of mammalian auditory nerve fibers show IF glides. Although the range of glides in mammals appears smaller than in the owl (14), it is sufficient to find pairs of monaural filters with mismatches in IF glide slopes and initial frequencies that would produce the experimentally observed dependence of best ITD on BF (*SI Materials and Methods*). The role of inhibitory inputs to MSO

neurons may thus be to shape the spectrotemporal tuning of monaural inputs, thereby affecting binaural mismatches. If inhibition creates binaural mismatches, then blocking inhibition would produce matched inputs and lead to best ITDs near zero, as observed (12). Our results thus suggest a mechanism by which inhibition could regulate ITD tuning that does not require precise timing. Testing this hypothesis will require developing methods to measure the monaural input to MSO cells.

We propose that a general framework for ITD computation is cross-correlation with spectrotemporally complex inputs. The interaction of the spectrotemporal properties of the monaural inputs can affect ITD computation to produce the observed responses in mammals and birds. The computation of ITD in birds and mammals may both be described using a common cross-correlation operation, with differences due to the degree of binaural spectrotemporal matching.

## Materials and Methods

Surgery, electrophysiology, and stimulus delivery have been described previously (13). Protocols followed National Institutes of Health guidelines and were approved by The Albert Einstein College of Medicine Animal Care and Use Committee. Briefly, six owls of both sexes were anesthetized by intramuscular injection of ketamine hydrochloride (20 mg/kg, Ketaject; Phoenix Pharmaceuticals) and xylazine (2 mg/kg, Xyla-Ject; Phoenix Pharmaceuticals). We recorded NL ($n$ = 27) neurons and NM neurons' axons entering NL ($n$ = 57) using a "loose patch" method (8, 36), allowing us to obtain stable recordings for >1 h. Earphones consisted of a speaker (Knowles 1914) and a Knowles 1939 microphone. At the beginning of each experiment, the earphones were automatically calibrated.

**Data Collection.** Data for reverse correlation were obtained by presenting binaurally uncorrelated 500-ms band-limited Gaussian noise (0.5–12 kHz) with an interstimulus interval of 500 ms. We collected 400 to 800 trials for each neuron. For each stimulus presentation, the signal was synthesized de novo to avoid correlation artifacts. The response to ITD vs. frequency was sampled in steps of 25 to 50 Hz.

**Reverse-Correlation Analysis.** The window of the reverse correlation was 10 ms (13). STAs were fit with gammatone, gabor, gammachirp, and gaborchirp filters, where the chirping filters had a linear IF glide (18). We fit the component of the STA where the envelope had >10% of its maximum value (18). The envelope of a signal $x$(t) is defined as the magnitude of the analytic signal $x$(t) + $iy$(t), where $y$(t) is the Hilbert transform of $x$(t). The gammatone and gabor filters are given by

$$g_{gammatone}(t) = A(t-t_0)^3 \exp(-(t-t_0)/\tau)\cos(2\pi f_0(t-t_0)+\phi)H(t-t_0) \quad [1]$$

$$g_{gabor}(t) = A\exp\left(-(t-t_0)^2/\tau\right)\cos(2\pi f_0(t-t_0)+\phi), \quad [2]$$

respectively, where $H$(t) is the unit step function. The gammachirp and gaborchirp filters are given by

$$g_{gammachirp}(t) = A(t-t_0)^3 \exp(-(t-t_0)/\tau)\cos\left(2\pi\left(f_0(t-t_0)+0.5c(t-t_0)^2\right)+\phi\right)H(t-t_0) \quad [3]$$

$$g_{gaborchirp}(t) = A\exp\left(-(t-t_0)^2/\tau\right)\cos\left(2\pi\left(f_0(t-t_0)+0.5c(t-t_0)^2\right)+\phi\right) \quad [4]$$

Fits were performed by minimizing a $\chi^2$ error $\chi^2 = \frac{1}{N-M}\sum_{n=1}^{N}\frac{(\mathrm{STA}(t_n)-g(t_n))^2}{\sigma_n^2}$, where $N$ is the number of time points, $M$ is the number of fit parameters, and $\sigma_n^2$ is an estimate of the variance of the STA at time point $n$ obtained from 1,000 bootstrap samples obtained with the Matlab (MathWorks) function bootstrp.

**Peak Frequency of Gammachirp Filter.** To determine the relationship between the BF of the gammachirp filter and the parameters $f_0$, $c$, and $\tau$, we produced 2,000 gammachirp filters by drawing parameter values from uniform distributions that covered the observed ranges. The relationship $\mathrm{BF} = f_0 + \pi c\tau$ explained 99% of the variance in BF.

**Cross-Correlation Model.** We examined the effect of an IF glide in impulse responses on the properties of binaural neurons using a cross-correlation model (13). An input signal is filtered with left and right gammachirp filters. The resulting signals are cross-correlated to give the model neuron response. The response of the cross-correlator neuron to ITD is given by

$$r(\mathrm{ITD}) = \frac{1}{T}\int_0^T [g_{left} * s(t-\mathrm{ITD})][g_{right} * s(t)]dt, \quad [5]$$

where $s(t)$ is the input stimulus, * represents the convolution operation, and $T$ is the time window.

We examined the effect of mismatches in the left and right ear input filters to the cross-correlation model on best ITD. We varied the left and right IF glides by using a range of values for the time constant and the IF glide slope. For 1,000 neurons at each BF, we generated left and right gammachirp filters by selecting the time constant and IF glide slope independently from a uniform distribution covering the observed range of values in NM. To fix BF, we modified $f_0$ to satisfy the relationship $\mathrm{BF} = f_0 + \pi c\tau$.

**Best ITD in NL.** We used the gammachirp fits to the monaural STAs to determine the contribution of interaural differences in delay and phase to the observed best ITD. We compared the best ITD found using the cross-correlation model having the fitted parameters with the best ITD found using the fitted parameters, but with equal IF glides. The IF glides were forced to be equal by setting the time constants $\tau$, IF glide slopes $c$, and instantneous frequencies at initial time $f_0$ to be equal to the values measured for the contralateral ear.

**STDP Model.** We tested whether an STDP rule could explain the spectrotemporal matching of monaural inputs in NL. The model consists of NL neurons receiving input from the left and right NM. Each NM neuron converts the output of a gammachirp filter into spike trains. Each individual filter is defined by three parameters: time constant $\tau$, IF glide slope $c$, and initial frequency $f_0$. The filters are normalized so that different sets of parameters produce the same spike rate. The output $x$ of the filter is first half-wave rectified to reflect phase-locking properties of auditory nerve firing (37, 38) and compressed by a one-third power law $I([x^+])^{1/3}$ (39, 40). The output is then fed to a leaky-integrate and fire (LIF) NM neuron

$$\tau_m\frac{dV(t)}{dt} = V_0 - V(t) + RI(t) + \sigma\sqrt{2\tau_m}\xi(t), \quad [6]$$

where $\tau_m = 0.3$ ms is the membrane time constant, $V_0 = -60$ mV is the resting potential, $R = 15\times10^{-3}$ohm is a constant, which includes the membrane resistance and the factor that converts the output of the filters into a current, $\xi(t)$ is Gaussian noise, and $\sigma = 0.085$ mV is the SD of the membrane potential in the absence of spikes. When $V$ crossed the threshold $V_t = -50$ mV, a spike is emitted and $V$ is reset to $V_r = -60$ mV and held for an absolute refractory period $t_{refrac} = 1$ms.

A total of 150 NL neurons with BFs randomly taken between 3 and 6 kHz are used for the training. NL neurons are also modeled as LIF neurons but their intrinsic noise $\sigma = 0.1$ mV is higher, their membrane time constant is $\tau_m = 0.1$ ms, and their inputs are synaptic: $I(t) = \sum_{ipsi} w_i S_i(t-\Delta_i) + \sum_{contra} w_i S_i(t-\Delta_i)$, where $S_i(t) = \sum_k \delta(t-t_i^k)$ is a train of $k$ spikes coming at times $t^k$ from synapse $i$, $w_i$ is the synaptic weight of synapse $i$, $\delta(t)$ is the Kronecker delta function, and $\Delta_i$ the conduction time from the ear via NM axon $i$ to NL. Before learning, each NL neuron receives an input population of 150 NM neurons from each side with the same BF. For each NL neuron, the 150 NM neurons are randomly drawn from a neuron "grid" of 25 × 60 = 1,500 possibilities. The grid axis with 25 elements is the axonal time delay and is linearly sampled between 0 and 150 μs. The grid axis with 60 elements is the parameters triplet axis, i.e., each point corresponds to certain values of $\tau$, $c$, and $f_0$. To be consistent with the measurements in NM, the $\tau$ values are randomly taken between 0.2 and 0.52 ms at each BF, whereas $c$ is drawn from an interval with boundaries varying linearly from [–0.3, 0.1] for BF = 3 kHz up to [0.2, 0.6] for BF = 6 kHz. Similarly, the interval boundaries for $f_0$ are [2.8 kHz, 3.4 kHz] for BF = 3 kHz up to [5.8 kHz, 6.4 kHz] for BF = 6 kHz.

In STDP, a synaptic change due to the co-occurrence of an input and an output spike takes place if the presynaptic spike arrival time and postsynaptic firing time both fall within a time window $W$ (25, 26). Here, $W$ is the window

extensively used in the literature (41) $W(\Delta t) = \left\{ \begin{array}{l} A_+ \exp(\Delta t/\tau_+) \, if \, \Delta t \geq 0 \\ -A_- \exp(\Delta t/\tau_-) \, if \, \Delta t < 0 \end{array} \right\}$. The parameters $\tau_+ = 0.05$ ms and $\tau_- = 3\tau_+ = 0.15$ ms determine the range of spike time intervals in which potentiation and depression of the synaptic weights occur; their values are of the order of the time constants encountered in the auditory brainstem, which is in accordance with previous studies (28, 30). The positive parameters $A_+$ and $A_-$ denote the maximum possible synaptic modification. Stable synaptic modification requires the integral of $W$ to be negative so that the STDP produces an overall depression. This condition means that the relationship $A_-\tau_- < A_+\tau_+$ holds. We set $A_+ = 5\times10^{-3}$ and $A_- = \frac{A_+\tau_+}{\tau_-}2 = 3.33\times10^{-3}$. To avoid unlimited growth, we impose an upper and lower bound on the weights: $w_i \in [0, w_{\max}]$ with $w_{\max} = 0.25$. The weights are randomly initialized between $0.05\,w_{\max}$ and $0.5\,w_{\max}$. All models were simulated with the Brian simulator (42), with a 5-μs time step. During the learning of each NL neuron, the filters at both ears received white noise with a fixed ITD, randomly taken from a Gaussian distribution centered on 0 μs with an SD of 50 μs. The learning simulations last 300 s, enough time for the firing rate and weights to stabilize. We used 30 s of binaurally uncorrelated white noise to compute the monaural STAs in trained neurons.

**ACKNOWLEDGMENTS.** This work was supported by National Institutes of Health Grant DC007690 (to J.L.P.), Marie Curie Team of Excellence Grant BIND MECT-CT-20095-02481 (to Sophie Deneve), and European Research Council Grant ERC StG 240132 (to R.B.).

1. Blauert J (1983) *Spatial Hearing: The Psychophysics of Human Sound Localization* (MIT Press, Cambridge, MA).
2. Moiseff A, Konishi M (1981) Neuronal and behavioral sensitivity to binaural time differences in the owl. *J Neurosci* 1:40–48.
3. Jeffress LA (1948) A place theory of sound localization. *J Comp Physiol Psychol* 41: 35–39.
4. Goldberg JM, Brown PB (1969) Response of binaural neurons of dog superior olivary complex to dichotic tonal stimuli: Some physiological mechanisms of sound localization. *J Neurophysiol* 32:613–636.
5. Carr CE, Konishi M (1990) A circuit for detection of interaural time differences in the brain stem of the barn owl. *J Neurosci* 10:3227–3246.
6. Yin TCT, Chan JCK (1990) Interaural time sensitivity in medial superior olive of cat. *J Neurophysiol* 64:465–488.
7. Shamma SA, Shen NM, Gopalaswamy P (1989) Stereausis: Binaural processing without neural delays. *J Acoust Soc Am* 86:989–1006.
8. Peña JL, Viete S, Funabiki K, Saberi K, Konishi M (2001) Cochlear and neural delays for coincidence detection in owls. *J Neurosci* 21:9455–9459.
9. Fischer BJ, Peña JL (2009) Bilateral matching of frequency tuning in neural cross-correlators of the owl. *Biol Cybern* 100:521–531.
10. Singheiser M, Fischer BJ, Wagner H (2010) Estimated cochlear delays in low best-frequency neurons in the barn owl cannot explain coding of interaural time difference. *J Neurophysiol* 104:1946–1954.
11. Joris PX, Van de Sande B, Louage DH, van der Heijden M (2006) Binaural and cochlear disparities. *Proc Natl Acad Sci USA* 103:12917–12922.
12. Brand A, Behrend O, Marquardt T, McAlpine D, Grothe B (2002) Precise inhibition is essential for microsecond interaural time difference coding. *Nature* 417:543–547.
13. Fischer BJ, Christianson GB, Peña JL (2008) Cross-correlation in the auditory coincidence detectors of owls. *J Neurosci* 28:8107–8115.
14. Carney LH, McDuffy MJ, Shekhter I (1999) Frequency glides in the impulse responses of auditory-nerve fibers. *J Acoust Soc Am* 105:2384–2391.
15. Recio A, Rich NC, Narayan SS, Ruggero MA (1998) Basilar-membrane responses to clicks at the base of the chinchilla cochlea. *J Acoust Soc Am* 103:1972–1989.
16. Irino T, Patterson RD (2001) A compressive gammachirp auditory filter for both physiological and psychophysical data. *J Acoust Soc Am* 109:2008–2022.
17. Shera CA (2001) Frequency glides in click responses of the basilar membrane and auditory nerve: Their scaling behavior and origin in traveling-wave dispersion. *J Acoust Soc Am* 109:2023–2034.
18. Wagner H, Brill S, Kempter R, Carr CE (2009) Auditory responses in the barn owl's nucleus laminaris to clicks: Impulse response and signal analysis of neurophonic potential. *J Neurophysiol* 102:1227–1240.
19. de Boer E, de Jongh HR (1978) On cochlear encoding: Potentialities and limitations of the reverse-correlation technique. *J Acoust Soc Am* 63:115–135.
20. Christianson GB, Peña JL (2007) Preservation of spectrotemporal tuning between the nucleus laminaris and the inferior colliculus of the barn owl. *J Neurophysiol* 97: 3544–3553.
21. Yin TCT, Chan JCK, Carney LH (1987) Effects of interaural time delays of noise stimuli on low-frequency cells in the cat's inferior colliculus. III. Evidence for cross-correlation. *J Neurophysiol* 58:562–583.
22. Bonham BH, Lewis ER (1999) Localization by interaural time difference (ITD): Effects of interaural frequency mismatch. *J Acoust Soc Am* 106:281–290.
23. Wagner H, et al. (2007) Distribution of interaural time difference in the barn owl's inferior colliculus in the low- and high-frequency ranges. *J Neurosci* 27:4191–4200.
24. McAlpine D, Jiang D, Shackleton TM, Palmer AR (1998) Convergent input from brainstem coincidence detectors onto delay-sensitive neurons in the inferior colliculus. *J Neurosci* 18:6026–6039.
25. Markram H, Lübke J, Frotscher M, Sakmann B (1997) Regulation of synaptic efficacy by coincidence of postsynaptic APs and EPSPs. *Science* 275:213–215.
26. Bi GQ, Poo MM (1998) Synaptic modifications in cultured hippocampal neurons: Dependence on spike timing, synaptic strength, and postsynaptic cell type. *J Neurosci* 18:10464–10472.
27. Tzounopoulos T, Kim Y, Oertel D, Trussell LO (2004) Cell-specific, spike timing-dependent plasticities in the dorsal cochlear nucleus. *Nat Neurosci* 7:719–725.
28. Gerstner W, Kempter R, van Hemmen JL, Wagner H (1996) A neuronal learning rule for sub-millisecond temporal coding. *Nature* 383:76–81.
29. Leibold C, Kempter R, van Hemmen JL (2001) Temporal map formation in the barn owl's brain. *Phys Rev Lett* 87:248101.
30. Kempter R, Leibold C, Wagner H, van Hemmen JL (2001) Formation of temporal-feature maps by axonal propagation of synaptic learning. *Proc Natl Acad Sci USA* 98: 4166–4171.
31. Guyonneau R, VanRullen R, Thorpe SJ (2005) Neurons tune to the earliest spikes through STDP. *Neural Comput* 17:859–879.
32. Rose JE, Gross NB, Geisler CD, Hind JE (1966) Some neural mechanisms in the inferior colliculus of the cat which may be relevant to localization of a sound source. *J Neurophysiol* 29:288–314.
33. Yin TCT, Kuwada S (1984) Neuronal mechanisms of binaural interaction. *Dynamic Aspects of Neocortical Function*, eds Edelman GM, Gall WE, Cowan WM (Wiley, New York), pp 263–313.
34. Qiu A, Schreiner CE, Escabí MA (2003) Gabor analysis of auditory midbrain receptive fields: Spectro-temporal and binaural composition. *J Neurophysiol* 90:456–476.
35. McAlpine D, Jiang D, Palmer AR (2001) A neural code for low-frequency sound localization in mammals. *Nat Neurosci* 4:396–401.
36. Peña JL, Viete S, Albeck Y, Konishi M (1996) Tolerance to sound intensity of binaural coincidence detection in the nucleus laminaris of the owl. *J Neurosci* 16:7046–7054.
37. Brugge JF, Anderson DJ, Hind JE, Rose JE (1969) Time structure of discharges in single auditory nerve fibers of the squirrel monkey in response to complex periodic sounds. *J Neurophysiol* 32:386–401.
38. Rose JE, Hind JE, Anderson DJ, Brugge JF (1971) Some effects of stimulus intensity on response of auditory nerve fibers in the squirrel monkey. *J Neurophysiol* 34:685–699.
39. Robles L, Ruggero MA (2001) Mechanics of the mammalian cochlea. *Physiol Rev* 81: 1305–1352.
40. Köppl C, Yates G (1999) Coding of sound pressure level in the barn owl's auditory nerve. *J Neurosci* 19:9674–9686.
41. Song S, Miller KD, Abbott LF (2000) Competitive Hebbian learning through spike-timing-dependent synaptic plasticity. *Nat Neurosci* 3:919–926.
42. Goodman DFM, Brette R (2009) The brian simulator. *Front Neurosci* 3:192–197.